

Influence of Two Rough Parallel Joint Surface Profiles on Stress Wave Energy Dissipation

Yexue Li^{1,2}, Hongke Pan^{1,3}, Li Qin¹ and Jianhui Fan¹

¹Hubei University of Arts and Science, Xiangyang 441053, China.

²Sichuan University, Chengdu 610065, China.

³Tongji University, Shanghai 200092, China.

E-mail: warmhearted520@sohu.com

ABSTRACT: A new method called YUV dimension is proposed to describe joint surface configuration on the basis of the interdisciplinary theory of iconography, graphics, and fractal geometry. This method can be used as substitute for traditional fractal dimensions. On this basis, the influence of two joint surface profiles (described by using the YUV dimension method) on stress wave energy dissipation is investigated by split Hopkinson pressure bar on embedded rough parallel two-joint rocks. The following conclusions are drawn: (1) the YUV dimension method, a new approach for characterizing surface configuration, exhibits more advantages than the traditional dimension; (2) the energy dissipation of the joints increases with increasing two-joint dimensions or their sums. This increase is attributed to the fact that the increase in YUV dimensions leads to the decrease in rock joint stiffness; thus, a decrease in rock joint stiffness leads to the increase in stress wave energy dissipation. A nonlinear relationship also exists among two YUV dimensions and energy dissipation. The nonlinear relationship is attributed to the nonlinear deformation of the joints. For engineering applications, a two-variable function between the energy dissipation and YUV dimensions of two joints is also formulated.

KEYWORDS: Energy dissipation, Stress wave, YUV dimension, Two joints, Surface configuration

1. INTRODUCTION

Statistical results from the state administration of work safety show that a large number of mining safety accidents occur in different provinces. These accidents include structure collapse, gas explosion, and flooding. The injury and death of workers resulting from these accidents involve thousands of persons each year. Direct economic damage is estimated to reach billions of dollars, whereas indirect economic damage is incalculable. Factors that lead to disasters cannot exclude human factors, such as loose regulation and insufficient safety awareness. However, a more typical reason is that our understanding of the energy transmission and dissipation principle of impact wave and stress wave formed by energy attenuation across many embedded jointed rocks during mining blasting excavation is far from complete. Thus, many engineering safety accidents occur during underground mining. These accidents cause immense economic and estate damages. Therefore, the effect of joints on stress wave energy dissipation should be investigated to minimize the engineering safety accidents and improve rock mass dynamic theory.

A study on the influence of joints on stress wave propagation generally applies the following methods. First, a constitutive model of joints is proposed or the existing constitutive model is applied directly. Second, an equation on stress and displacement of stress wave crossing the joints is established on the basis of displacement discontinuity model. Solving the equation leads to the obtainment of the analytical solutions of transmission and reflection coefficients and the energy dissipation of the stress wave. Only elastic deformation occurs in the joint affected by the stress wave when the stress amplitude is low. Joint deformation is linear elastic; thus, solving the transmission and reflection coefficients of stress wave is relatively simple. However, a stress wave with high amplitude causes nonlinear joint deformation. Traditional linear constitutive relationship cannot be used to describe the relationship between the stress and strain of joints with nonlinear deformation characteristic. Thus, the linear constitutive relationship must be replaced with the nonlinear constitutive relationship. The nonlinear constitutive relationship previously applied is called the hyperbola (or BB) model (Bandis et al., 1983). The analytical solution of the transmission and reflection coefficients of stress wave across the joint is derived by using the constitutive relationship (Yu, 2008). However, the BB model reveals the relationship between the stress

and strain of the joint under static loading. The static constitutive relationship that has been applied to investigate the dynamic problem easily results in deviation or even error. To overcome this flaw, a dynamic BB model (Zhao et al., 2008) is presented by impact loading experiments on jointed rock. The UDEC numerical solution of the transmission and reflection coefficients of stress wave was estimated by introducing the dynamic BB model. A subsequent study (Yu et al., 2009) has found that the BB model proposed in the previous study (Zhao et al., 2008) has an inherent defect. The study proposed a three-parameter model, i.e., an improved nonlinear normal constitutive relationship by defining a new maximum allowable closure to be added to the model. The approximate analytical solution of transmission and reflection of stress wave across a single joint is derived on the basis of improved constitutive relationship. A rock mass formed by thousands and thousands of years of geotectonic movement contains a large number of joints. Thus, the influence of multiple parallel nonlinear joints on stress wave is investigated, and the analytical solution of the transmission coefficient is derived on the basis of the displacement discontinuity model (Cai and Zhao, 2008).

Previous studies are based on a common assumption that the joint surface is a smooth plane. It is only based on the assumption that the incident angle can be determined accurately. In fact, a natural joint is a rough surface. If the joint is considered an aggregate of micro segments, the incident angles of stress wave incident on each microsegment vary. Therefore, determining the incident angle of the stress wave across the aggregate, i.e., the entire joint, is difficult. As such, investigating the analytical solution of the stress wave across the rough joint surface is also difficult. Moreover, the linear and nonlinear constitutive relationships of the joints both include *JRC* (Barton, 1978), a parameter used to characterize joint surface configurations. Nevertheless, the *JRC* parameter is an empirically estimated value obtained by comparing the tested curve with the standard curve. The *JRC* parameter is also used to describe the curved line profile but not the curved surface profile. Therefore, directly applying the parameter to characterize the curved surface configuration, such as the joint surface configuration, is inappropriate.

Fractal theory is an effective theoretical tool and a practical engineering method used to describe surface configuration. Since Mandelbrot (Mandelbrot, 1967) proposed the fractal theory in 1973, the calculation theory of fractal dimension has undergone various

stages of development from triangular prism surface area (Clarke,1986), projected coverage (Xie and Wang,1999), cubic covering method (Zhou and Xie,2003), and improved cubic covering method (Zhang and Zhou, 2005) to the volume covering method (Zhou et al., 2014). Considering the narrow scanning scope of a laser profilometer for gathering the 3D coordinates of a rough surface compared with the size of engineering rock mass, researchers have proposed several indirect calculation methods, such as binary image dimension, grayscale image dimension (Pentland, 1984), and true-color image dimension (Li and Gao, 2012). These studies show that all aforementioned dimensions are self-similar. However, A rough rock surface or terrain in the direction vertical to the surface is self-affine (Xie, 1993). Thus, probing into image self-affine dimension theory has considerable theoretical implications and practical engineering values.

The objective of this study is to investigate the influence of two rough parallel joint surface profiles on stress wave energy dissipation. First, the YUV dimension method is proposed to characterize joint surface roughness. Second, the influence of joint surface roughness on stress wave energy dissipation is estimated on the basis of the proposed method. Finally, the quantitative relationship between two rough parallel joint surface self-affine dimensions, namely, YUV dimension and stress wave energy dissipation, is established.

The main contents of this study comprise the following three parts: (1) the YUV dimension method is proposed and all joint surface YUV dimensions are evaluated; (2) on the basis of the incident wave, reflected wave, and transmitted wave collected by the split Hopkinson pressure bar (SHPB) experiment on an embedded rough parallel two-joint rock sample, the energy dissipation of the stress wave across the joint is calculated. The energy dissipation characteristic is also analyzed by using the time-domain curves; (3) the MATLAB toolbox is applied to establish a two-variable function of energy dissipation by considering the effect of the two rough parallel joint surface profiles.

2. PROCESSING THE EMBEDDED ROUGH PARALLEL TWO-JOINT ROCK SAMPLE

Given that this study aims to determine the influence of two artificial joints on stress wave propagation, side effects from discontinuous interfaces in rock samples, such as natural pores or cracks, on the experimental result should be avoided. Therefore, marble with compact structures and pure grain are used in the experiment. A rock core with a diameter of 50 mm and a length of 80 mm is drilled from the rock mass by using a standard rock cutter. Given that several mechanical properties of a rock are anisotropic, rock coring should be conducted in a similar direction to prevent side effects from anisotropies of rock parameters on the experimental result. After the two bottoms of the rock core are polished crudely, the rock core is cut twice perpendicular to its axis. The joint surface of the semi-finished rock sample is scotched along different directions to create a rough surface. The objective of this process is to simulate the roughness of a natural joint surface. After the rough joint surface is photographed by a DP digital camera, three separate parts are cemented with AB glue. The semi-finished rock sample is then carefully polished until the parallelism and planeness required in the experiment are satisfied. Finally, 28 embedded two-joint rock samples with a length of 65 mm and a diameter of 50 mm are manufactured. In all manufactured samples, other parameters are the same, except for the YUV dimensions of the two joint surface configurations (Figure 1).

3. ANALYZING THE PROFILE CHARACTERISTIC OF THE JOINT SURFACE

Previous studies showed that the fractal characteristic of the rock joint surface and its surface image is the same [13] and that the fractal characteristic of the surface profile is not self-similar but self-

affine [15]. Thus, It is inappropriate that traditional fractal dimension method used to analyze the self-similar fractal characteristic is applied to probe into self-affine fractal characteristic. The current study proposes a new image fractal dimension method called YUV dimension on the basis of the interdisciplinary theory of iconography and graphics, as well as fractal geometry. The YUV dimension is applied to characterize the rough characteristic of the rock sample joint surface.

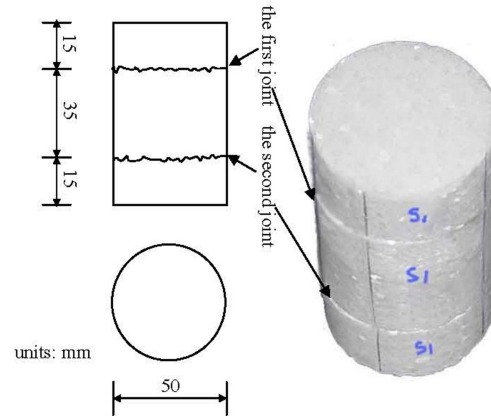


Figure 1 Image and schematic figure of the rock sample with two rough parallel joints

3.1 A New Method Called YUV Dimension for Describing Joint Surface Profiles

3.1.1 Acquiring the 3D Coordinates of the Rough Surface

RGB is generally the selected color space used to describe the color property of the rock sample digital photo. Nevertheless, on the basis of the requirement of investigating the fractal characteristic of the image, one of the three color components in the selected color space must explicitly denote the grayscale of the image color. All three components must be orthogonal to one another. Thus, the YUV color model is applied to describe the color characteristic in this study. After the color space is converted from RGB to YUV, a 3D vector can be established in the coordinate system that originates from the pixel point (see **A1A** and **B1B** in Figure 2).

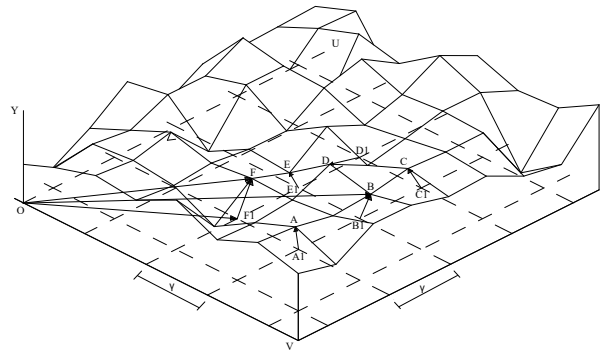


Figure 2 Diagram of the YUV surface topography

The pixel is set as the origin of the coordinate system. Thus, the vector(see **F1F** in Figure 2) can be expressed as follows:

$$F_1F = U_1\mathbf{u} + V_j\mathbf{v} + Y_{i,j}\mathbf{y}, \quad (1)$$

where U_i , V_j , and $Y_{i,j}$ are the color components of point F_1 described by using the YUV color model. By unifying the vector into the coordinate system that originates from point O , the vector can be expressed as follows:

$$\mathbf{OF} = (U_i + m\gamma)\mathbf{u} + (V_j + n\gamma)\mathbf{v} + Y_{i,j}\mathbf{y}, \quad (2)$$

where γ is the side length of the grid cell, i.e., pixel interval; m and n are the number of grid cells along the U and V axes, respectively. Given the randomness of the vectors, the coordinates of the point on the surface can be expressed as $\{U_i + m\gamma, V_j + n\gamma, Y_{i,j}\}$ in the unified coordinate system.

3.1.2 Calculating the YUV Dimension

From the numerical characteristics of the fractal Brownian motion, the following equations are obtained:

$$\text{Var}[B_\alpha(X+H) - B_\alpha(X)] \propto \|H\|^{2\alpha}, \quad (3)$$

$$E[B_\alpha(X+H) - B_\alpha(X)] = 0, \quad (4)$$

where $B_\alpha(X)$ is the fractal Brownian function; H is the $n - 1$ dimensional vector; Var is the variance sign; E is the expectation operator and α denotes the Hurst index. Thus,

$$E[B_\alpha(X+H) - B_\alpha(X)]^2 \propto \|H\|^{2\alpha} \quad (5)$$

The proportional coefficient is selected, and the logarithm of the equation is calculated. The following equation is then obtained:

$$\alpha = \frac{\log\{E[B_\alpha(X+H) - B_\alpha(X)]^2\}}{\log\|H\|^2}. \quad (6)$$

On the basis of the relationship between the Hurst index and fractal dimension, the following formula can be obtained:

$$D = n - \alpha, \quad (7)$$

where D is the YUV dimension. The rough rock surface is 3D in Euclidean space. Thus, the value of variable n is three. By substituting Eq. (6) into Eq. (7), the following equation can be derived:

$$D = 3 - \frac{\log\{E[B_\alpha(X+H) - B_\alpha(X)]^2\}}{\log\|H\|^2}. \quad (8)$$

By considering the special research object, i.e., rough rock surface, the physical meaning of Eq. (8) is that $E[B_\alpha(X+H) - B_\alpha(X)]^2$ reflects the average of the square of the height difference between two points (or the grayscale difference) on the rough surface. $\|H\|^2$ denotes the square of the distance of the two projective points on the plane.

3.2 Analysis of the Fractal Characteristic of the Rough Rock Surface Based on the YUV Dimension Method

The rough rock surface is photographed by using a high-resolution digital camera. The largest rectangular region image is intercepted from the circular cross-section image for the subsequent calculation of the YUV dimensions. The 3D coordinates of the intercepted image are obtained on the basis of the method described in Section 3.1.1. The figure of the rough rock surface configuration is drawn by inputting the 3D coordinates into Surfer 8.0, which is a type of commercial software used to plot terrain figures. On the basis of the YUV dimension method, a software is programmed by using MATLAB (a high-performance computer programming language) to estimate the YUV dimensions of the rough surface. Thereafter, the YUV dimensions of all rock samples are evaluated and the corresponding bi-logarithm figures are plotted. Two groups of typical figures on the rough surface photo, its configuration, and the corresponding bi-logarithm plot are illustrated in Figure 3.

The rough surface image shows that crisscrossing nickels exist on the rough surface of sample S1 and S6. Moreover, the rough surface of sample S6 appears to be rougher than that of sample S1. The fine structure of S6 seems to be more than that of sample S1. The corresponding rough surface configuration of the samples also indicates that the nickels in the horizontal and longitudinal directions intersect. The nickels of sample S6 appears to be deeper than those of S1. Nickels with different widths are also distributed more irregularly. Thus, the entire profile of sample S6 seems to be rougher than sample S1. This finding shows that the photo and drawn configuration figure have nearly similar profile characteristics. The changing principles of their roughness degrees are also fundamentally consistent.

The presented analysis is qualitative. Subsequently, a quantitative investigation is conducted. The bi-logarithm plot of the YUV dimension shows that the YUV dimension of samples S1 and S6 are 2.65827 and 2.84139, respectively. The YUV dimension of sample S6 is greater than that of sample S1. A comparison of the qualitative analysis and quantitative investigation indicates that the YUV dimension calculated is high when the surface is rough and vice versa. This result shows that the YUV dimension method and precondition on which the method is based are reasonable and feasible. The new image dimension can be used as substitute for traditional fractal dimensions to characterize surface configuration.

3.3 Comparative Analysis between the YUV Dimension and the Traditional Dimension

Surface profile data of Sample S1 and S6 are acquired by the laser profilometer showed in Figure 4. The software programmed in the paper is applied to calculate the YUV dimension based on data by the laser profilometer scanning jointed rock surface. Bi-logarithm plots on YUV dimension are illustrated in Figure 3.

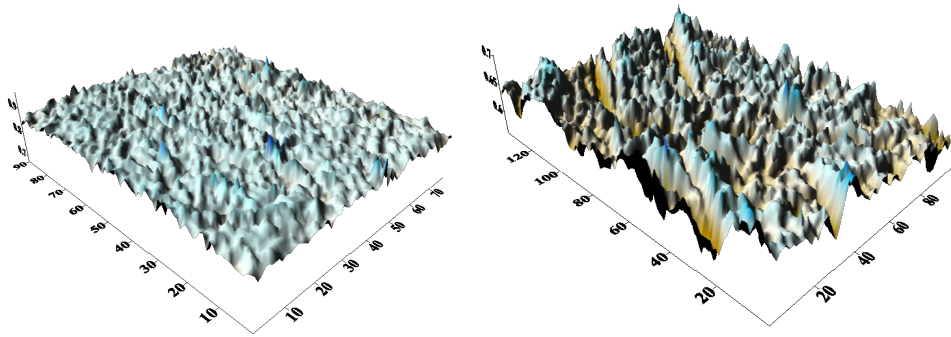
Two kinds of dimension from Sample S1 and S6 are compared in Figure 3. It is clear that their YUV dimensions increase from 2.65827 to 2.84139. Meanwhile Self-affine dimensions evaluated by scanning data of the laser profilometer also increase from 2.59124 to 2.62396. Obviously, rising of surface roughness showed in surface profile figure leads to the increasing of two kinds of dimensions. It is indicated that YUV can characterize the jointed rock surface roughness similar to traditional self-dimension.

Additionally, The YUV dimension based on fractal Brownian function has the following advantages.

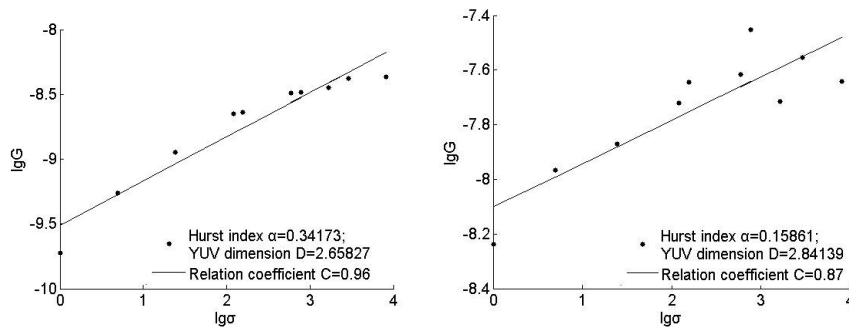
- (1) The traditional image dimension is a self-similar dimension. However, the fractal property in the direction vertical to the joint surface is self-affine. Therefore, the use of the YUV dimension based on self-affine theory to characterize the rock joint surface configuration is more appropriate than the traditional image dimension based on self-similar theory.



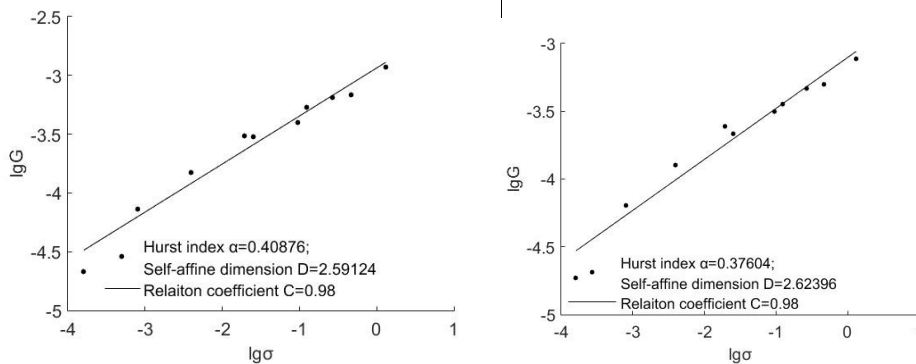
S1 Figure of the rough surface image of the first joint S6



S1 Figure of the rough surface profile of the first joint S6



S1 Figure of the bi-logarithm plot of the first joint S6



S1 Figure of the bi-logarithm plot of the first joint based on data acquired by the laser profilometer S6

Figure 3 Photograph, profile, and bi-logarithm figure of the first joints of samples S1 and S6

- (2) If the traditional fractal dimension is evaluated, a laser profilometer should be applied to gather the 3D coordinates of the rock joint surface. However, in the method proposed in this paper, the device that must be needed in the experiment is only a digital camera used to shoot the photo of the rock joint surface. This method costs less than the traditional method during the experiment and makes the experiment operation simple.

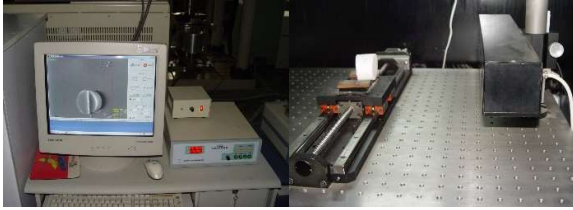


Figure 4 Laser profilometer

4. ENERGY DISSIPATION PRINCIPLE OF STRESS WAVE ACROSS TWO ROUGH PARALLEL JOINTS

The time-domain curves are analyzed to investigate the energy dissipation principle of the stress wave by the SHPB experiment on an embedded two-joint rock sample. The quantitative relationships between the energy dissipation of the stress wave and two YUV dimensions, as well as those between the energy dissipation and YUV dimension sums, are established.

4.1 SHPB Experiment on an Embedded Two-joint Rock

The jointed rock is installed between the input and output bars (see Figure 5). The striker bar, driven by high-pressure gas, impacts the input bar at a velocity of 9.3 m/s to trigger a stress impulse $\sigma(t)$. The stress impulse, which is also called the incident wave, propagates forward in C_e speed and recorded by strain gauge 1. With the passage of L_e/C_e time interval (where L_e is length of the input bar), the incident wave reaches the A1 interface between the input bar and the rock sample. Given their wave impedance differences, the wave is simultaneously reflected and transmitted on the interface. The transmission wave continues to propagate forward. When the transmission wave encounters the first joint, complicated transmission and reflection occurs; the wave type also changes as a result of the joint roughness degree and wave impedance differences between the joint and rock. The propagated transmission wave subsequently encounters the second joint. Thereafter, the transmission and reflection phenomena similar to that in the first joint occur. Nevertheless, the stress wave field on the second joint is more complex than that on the first joint. When the stress wave continues to propagate and arrives at interface A2, the transmission and reflection phenomena are also triggered synchronously. The impulse only lasts $2L_s/C_s$ seconds and passes back and forth the rock sample for one time (where L_s and C_s are the rock sample length and velocity of the wave propagating in the sample, respectively). The time interval is approximately several microseconds. The stresses and strains between the rock sample and two bottoms are fundamentally consistent after several times of transmission and reflection of the stress wave. At the end of the aforementioned process, stress impulses $\sigma_r(t)$ (the reflected wave in the input bar) and $\sigma_t(t)$ (the transmitted wave) are recorded by strain gauges 1 and 3, respectively.

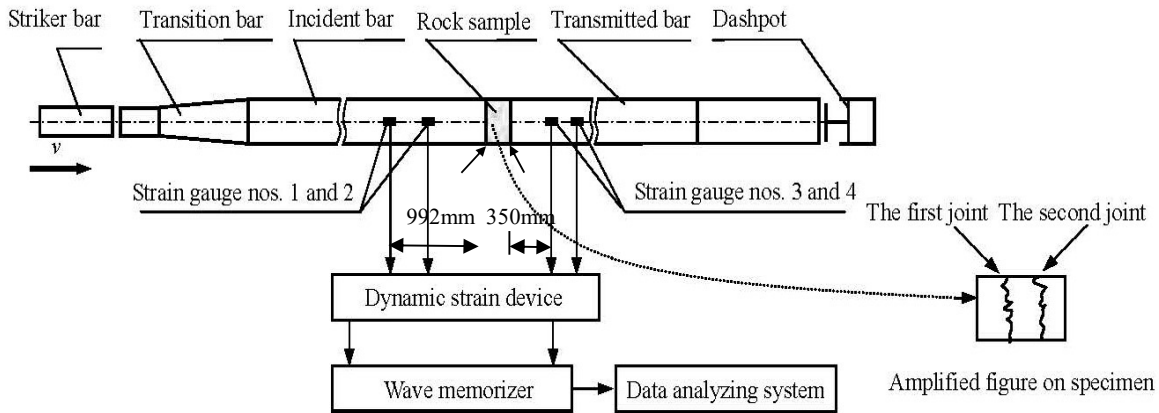


Figure 5 SHPB device

4.2 Analysis of the Energy Changing Principle of the Stress Wave Based on the Time-domain Curve

To ensure comparability among the results from different samples, an impact speed of approximately 9.3 m/s is set in the study to input similar waveform and energy into different rock samples. To focus on the effect of rough joint surface profile on stress wave energy dissipation, the other parameters are manufactured to be the same, except for the YUV dimensions of the two artificial joints in all samples (Figure 1). The two bottoms of the samples are smoothed and greased to minimize disturbance from friction between the sample and bars. Twenty-eight groups of incident wave, transmitted wave across the joint, and reflected wave that bounced from the joint during impact loading are recorded. The waveform figures of

the incident wave, transmitted wave, and transmitted wave of samples S1 and S6 are illustrated in Figure 6. These waveform figures show the following results.

- (1) The high-frequency oscillation phenomenon in the reflected wave is more remarkable than those in the incident and transmitted waves.

A reshaper is applied to change the incident waveform from a rectangular wave to a triangular wave to minimize the inertia dispersion effect. Although the high-frequency oscillation phenomenon remains in the incident wave, the phenomenon is not notable compared with that in the reflected wave. Moreover, a comparison shows that the phenomenon in the reflected wave is also more evident than that in the transmitted wave. A possible reason is that the nonlinear deformation of the joints embedded in the rock

leads to a high-frequency wave under impact loading and is accompanied by the high-frequency oscillation phenomenon. The information should be carried not only in the reflected wave but also in the transmitted wave. However, the filtering function of the joint enables some high-frequency waves in the transmitted wave to be filtered. Thus, the high-frequency oscillation in the reflected wave is more remarkable than that in the transmitted wave in the experiment.

(2) The energy of the reflected wave is remarkably larger than that of the transmitted wave.

The calculation from the stress versus time curves for samples S1 and S6 shows that the input energies of their incident waves are 1925 and 2,105 J, whereas the corresponding energies of the reflected waves are 867 and 1,021 J, respectively. The energy ratios of their reflected wave to that of their incident wave are 23% and 17%, respectively. The corresponding energies of the transmitted waves are 205 and 174 J, respectively. The proportions of energy to that of the incident wave are 10% and 8%, respectively. Obviously, most of the energy is reflected back to the input bar. Only a minimal amount of the energy passing through the joints continuously propagates forward, except for the energy of the stress wave that is dissipated by joints as plastic deformation energy and surface energy. The existence of the joint remarkably weakens the jointed rock stiffness. When the joint stiffness is weak, the energy that crosses the joint is small. By contrast, the energy reflected back is comparatively large. This finding indicates that the jointed rock stiffness is a determining factor of the energy of the transmitted wave.

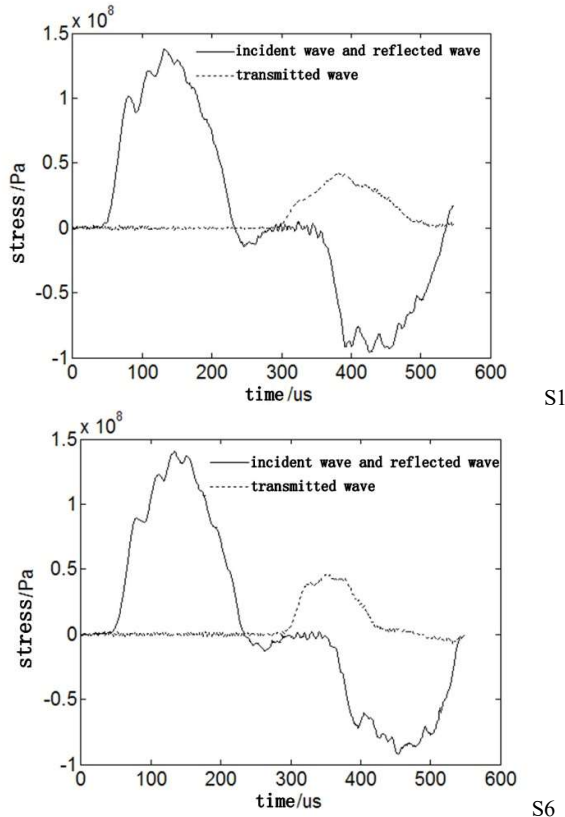


Figure 6 Stress wave waveform of the jointed rock

4.3 Analysis of the Influence of the Two Joint Surface Profiles on the Energy Dissipation of the Stress Wave

When the dynamic constitutive relationship of the rock is investigated by using the SHPB testing technique, the stresses in the

input bar, output bar, and rock sample must be in a strictly 1D condition. However, when the technique is applied to investigate the energy dissipation principle of jointed rock, only the input and output bars are required to be in the 1D stress state. Energy dissipation can be evaluated by calculating the difference between the input and output bar energies. The aforementioned study shows that the incident wave, reflected wave propagating in the input bar, and transmitted wave propagating in the output bar are in a 1D stress state. Therefore, a uniform formula for calculating energy can be expressed as follows:

$$W = \int_0^T A\sigma(t)C\varepsilon(t)dt, \quad (9)$$

where W is the energy of the stress wave; T denotes the time interval spent on stress wave propagation; $\sigma(t)$ refers to the stress wave propagating in the bar; C is the stress wave velocity, and $\varepsilon(t)$ refers to the strain wave propagating in the bar. Hooke's law states that a steel bar in the 1D elastic deformation condition satisfies the following constitutive relationship:

$$\sigma(t) = E\varepsilon(t), \quad (10)$$

where E is the Young's modulus of the steel bar. By substituting Eq. (10) into Eq. (9), we can derive the following equation:

$$W = \frac{AC}{E} \int_0^T \sigma^2(t)dt. \quad (11)$$

In a homogeneous elastic steel bar, the propagation speed can be expressed as follows:

$$C = \sqrt{\frac{E}{\rho}}, \quad (12)$$

where ρ is the volume density. The previous formula is rewritten by substituting Eq. (12) into Eq. (11). Thus, the following equation can be obtained:

$$W = \frac{A}{C\rho} \int_0^T \sigma^2(t)dt. \quad (13)$$

Eq. (13) is the uniform formula to calculate the energies of the incident, transmitted, and reflected waves. Thus, the equation set to evaluate corresponding energy is obtained by substituting the corresponding stress wave function $\sigma(t)$:

$$\begin{cases} W_i = \frac{A}{C\rho} \int_0^T \sigma_i^2(t)dt \\ W_r = \frac{A}{C\rho} \int_0^T \sigma_r^2(t)dt, \\ W_t = \frac{A}{C\rho} \int_0^T \sigma_t^2(t)dt \end{cases} \quad (14)$$

where W_i , W_t , and W_r are the energies of the incident, transmitted, and reflected waves, respectively; $\sigma_i(t)$, $\sigma_t(t)$, and $\sigma_r(t)$ are the incident, transmitted, and reflected waves, respectively. The dissipated energy induced by impact loading mainly includes three parts, namely, the plastic strain energy caused by the nonlinear

deformation of jointed rock, the surface energy dissipated by the expansion of cracks and formation of new surfaces, and the kinetic energy carried by bounced or popped jointed rock sample and other energies, such as acoustic, thermal, and radiant energies. The aforementioned study shows that the proportion of other energies to total dissipated energy is significantly low at less than 5%. Moreover, the impact speed of the striker bar is strictly controlled at less than 10 m/s. This speed is comparatively slow. The phenomenon that the sample is bounced or popped is not observed in the experiment. Therefore, the dissipated energy from kinetic energy is relatively low and can be omitted on the precondition of an insignificant side effect on the research conclusion. Thus, on the basis of the law of energy transformation and conservation, the energy dissipated by the jointed rock can be approximately obtained as follows:

$$W_d = W_i - W_r - W_t \tag{15}$$

By substituting the energy equation set in Eq. (14) into Eq. (15), the following equation can be obtained:

$$W_d = \frac{A}{C\rho} \left[\int_0^T \sigma_i^2(t)dt_1 - \int_0^T \sigma_r^2(t)dt \right] - \int_0^T \sigma_i^2(t)dt \tag{16}$$

On the basis of the jointed rock energy dissipation calculation theory, Eq. (16) was applied to program the software to calculate energy dissipation using MATLAB. The energy and energy dissipation of 28 jointed rocks are estimated.

For application in the field of rock and soil engineering, the study employs Sftool (a function package for fitting 3D data) in MATLAB 2010 to program the regression analysis software to establish the relationship between the energy dissipation of the stress wave and two joint YUV dimensions D_1 and D_2 . The two-variable function relationship among the three parameters is fitted by inputting the two YUV dimensions and corresponding energy dissipation into the software. The tendency of energy dissipation is formulated in terms of the YUV dimensions of the two joints as follows:

$$ED = 514.8 \exp(0.42D_1) + 2.25 \exp(1.55D_2) - 690.2 \tag{17}$$

The fitted curved surface describing the relationship among the three parameters is also plotted in Figure 7 to show the variations of the principle of energy dissipation with the change of two YUV dimensions.

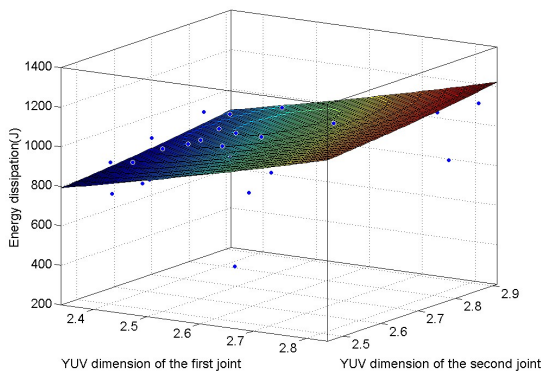


Figure 7 Relationship between two joint YUV dimensions and energy dissipation

The following observations are noted:

- (1) The regressed curved surface figure and fitted formula imply that energy dissipation increases with the increasing YUV dimension of the other joint when the YUV dimension of one joint remains invariant. The energy dissipates more rapidly with the simultaneous increase in the two-joint YUV dimensions than that with the single-joint YUV dimension. This finding can be explained by joint stiffness. With the increase in YUV dimension, e.g., increase in roughness of the jointed surface, the corresponding joint stiffness decreases. Thus, the capacity of the stress wave crossing the joint decreases. The energy attenuated by the joint also increases. If the YUV dimensions of the two joints increase synchronously, the corresponding joint stiffness decreases in more rapid speed, and thus the dissipated energy is more than that of a single joint.
- (2) The fitted formula and tendency of the curved surface show that energy dissipation varies nonlinearly with the change in the other YUV dimensions when one YUV dimension remains fixed. Moreover, the fitted function between the energy dissipation of the stress wave and YUV dimensions of two joints is also nonlinear. A nonlinear relationship exists among the three parameters and is possibly induced by the nonlinear deformation of jointed rocks under the condition of impact loading.

The tendency of energy dissipation to increase with the sum of the YUV dimensions of two joints has been plotted in Figure 7 on the basis of the data on energy, energy dissipation of the stress wave, and YUV dimensions of the jointed rock. The triangular symbol in the figure denotes the energy dissipation of the jointed rock; the rectangular symbolizes the energy carried by the transmitted wave; the solid line denotes the tendency of the energy of the transmitted wave; the dashed line shows the tendency of energy dissipation. Figure 8 reveals that the energy dissipation of the jointed rock or the energy of the transmitted wave fluctuates. Nevertheless, their total tendency is clear. The energy dissipation of the jointed rock increases with the increasing YUV dimensions of the two joints. In contrast to the aforementioned principle, the energy of the transmitted wave decreases with the increasing YUV dimensions of the two joints. The possible cause can be explained as follows: the relationship between the joint stiffness and fractal dimension of the joint surface reveals that the corresponding joint stiffness decreases when the joint fractal dimension increases. Therefore, the increase in YUV dimension leads to the decrease in the joint stiffness of the corresponding sample. Furthermore, the decrease in joint stiffness results in the increase in the capacity of the joint to attenuate energy and the decrease in the probability of the stress wave to propagate through the joint.

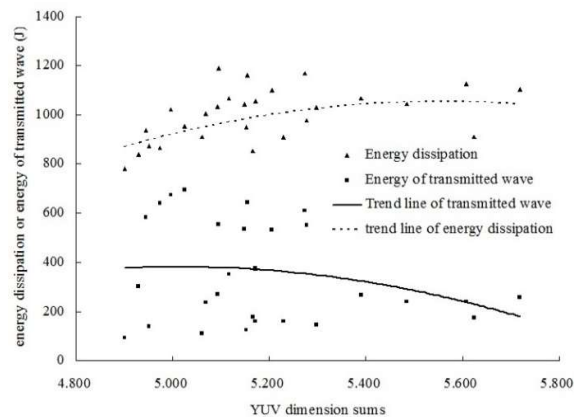


Figure 8 Relationship between dimension and dissipation

5. CONCLUSIONS

This study has investigated the influence of the surface configuration of two joints on stress wave energy dissipation on the basis of the interdisciplinary theory of fractal geometry, iconography and graphics, as well as rock dynamics. The following conclusions are obtained.

- (1) A new YUV dimension method that can substitute for traditional fractal dimensions is presented to characterize surface configuration. According to numerical analysis and comparison with laser profilimeter scanning experiment, the method and presumption are feasible and reasonable.
- (2) The increase in either of the two YUV dimensions leads to the increase in the corresponding dissipated energy. An approximate nonlinear relationship exists between the YUV dimensions and energy dissipation. The nonlinear relationship is triggered by nonlinear deformation during impact loading.
- (3) The total tendency of the transmitted wave energy gradually decreases with the increasing YUV dimensions of the two joints. By contrast, the total tendency of the dissipated energy of the two joints increases with increasing YUV dimensions. This finding can be attributed to the decrease in joint stiffness with increasing YUV dimension; the decrease in joint stiffness increases the capacity of the joint to attenuate stress wave energy and decreases the probability of the stress wave to propagate through the joint.
- (4) The high-frequency harmonic wave phenomenon is induced by nonlinear deformation under impact loading on jointed rock. The joint filters the high-frequency wave, which phenomenon will occur depends on the basic characteristic parameters of the stress wave and the relative dynamic property of the jointed rock.

6. ACKNOWLEDGMENTS

This work has been funded by the National Natural Science Foundation of China (Grant No. 51374100), the Natural Science Foundation of Hubei Provincial department of education of China (Grant No. D20142603).

7. REFERENCES

- A.P.Pentland. Fractal-based description of natural scenes[J].IEEE PAMI, 1984,6(6):973-981.
- Bandis S C, Lumsden A C, Barton N R. Fundamentals of rock fracture deformation[J]. International Journal of Rock Mechanics and Mining Sciences and Geomechanics Abstracts, 1983,20(6):249-268.
- Barton N R. Suggested method for the quantitative description of discontinuities in rock masses [J]. Int. J. Rock Mech. Min. Sci.1978,15(6):319-368.
- Clarke, K. C. Computation of the fractal dimension of topographic surfaces using the triangular prism surface area method[J]. Comput. Geosci, 1986,12(5):713-722.
- H.P.Xie., Wang,J.A. Direct fractal measurement of fracture surfaces. Int. J Solids Struct. 1999 ,36(20): 3073-3084.
- H.P.Xie. Fractals in Rock Mechanics[M]. Rotterdam : A. A. Balkema , 1993.
- H.W. Zhou, D.J. Xue, D.Y. Jiang. On fractal dimension of a fracture surface by volume covering method. Surface Review and Letters, 2014, 21(1), 1450015.
- H. W. Zhou, H. XIE. Direct estimation of the fractal dimensions of a fracture surface of rock [J]. Surf. Rev. Lett. 2003,10(5): 751-762.
- J. G. Cai, J. Zhao. Effects of multiple parallel fractures on apparent attenuation of stress waves in rock masses [J]. International Journal of Rock Mechanics and Mining Sciences 37 (2000) 661-682.

- J. Yu, Q. Qian, Z.M.Lin. Study on p-waves across improved single fracture with nonlinear normal deformation behavior[J]. Chinese Journal of Geotechnical Engineering, 2009,31(8):1156-1164.(in Chinese)
- J. Yu. Effects of Single Joint with Different Nonlinear Normal Deformation Behaviors on P-wave Propagation. Proceedings of the 2nd International Conference On Geotechnical Engineering for Disaster Mitigation and Rehabilitation.2008: 458-465.
- J. Zhao, J. G. Cai, X. B. Zhao, and H. B. Li. Dynamic Model of Fracture Normal Behavior and Application to Prediction of Stress Wave Attenuation Across Fractures [J]. Rock Mech. Rock Eng. 2008,41 (5), 671-693.
- Mandelbrot B B. How long is the coastline of Britain? Statistical self-similarity and fractal dimension[J]. Science , 1967,155(4): 636-638.
- Y.X.Li, M.Z.Gao. Study on IFD Calculated Theory and Nature of True color Image, Surface Review and Letters ,2012,19(3): 1250031-1250043.
- Zhang Ya-heng , Zhou Hong-wei , XIE He-ping. Improved cubic covering method for fractal dimensions of a fracture surface of rock. Chinese Journal of Rock Mechanics and Engineering [J]. 2005,24(17):3192-3196. (in Chinese)